J MATER SCI 41 (2006) 2611–2614

Structural characterization of iron silicides nanoparticles grown on Si substrate: Annealing rate dependence

J. H. WON*
Department of Materials Science and Engineering, Osaka University, Suita, Osaka 565-0871, Japan
E-mail: jhwon22@sanken.osaka-u.ac.jp
K. SATO, M. ISHIMARU, Y. HIROTSU
The Institute of Scientific and Industrial Research, Osaka University, Ibaraki, Osaka 567-0047, Japan

We have synthesized iron silicides on a Si(111) substrate using an electron-beam evaporation technique in combination with thermal annealing. The microstructures, as a function of heating rate on annealing, were characterized by transmission electron microscopy (TEM). Bright-field plan-view TEM observations revealed that a discontinuous thin film is formed in the sample annealed rapidly, while complete separated nanoparticles were obtained in the specimen annealed slowly. Selected-area and nano-beam electron diffraction patterns indicated that the former and latter specimens mainly consist of iron monosilicide (ε-FeSi) and iron disilicide (β-FeSi$_2$) phases, respectively. © *2006 Springer Science + Business Media, Inc.*

1. Introduction

Fe–Si binary compounds are environmentally friendly materials because of their abundant existence on the earth and lack of chemical pollution. Among the various different compounds, β-FeSi$_2$ has attracted much attention due to its excellent physical properties such as a direct band gap of 0.8–0.85 eV [1, 2] and large optical absorption [3] and Seebeck coefficients. In addition, this material can be epitaxially grown on a Si substrate [4]. Therefore, β-FeSi$_2$ is one of the candidate materials for Si-based optoelectronic devices and thermoelectric conversion applications such as solar cells [5].

Previous experimental and theoretical studies [6, 7] reported that strain in β-FeSi$_2$ plays an important role in its light-emitting properties. The formation of β-FeSi$_2$ nanoparticles is a possible way to control the strain. Electron-beam evaporation is a useful technique for forming nanoparticles. In fact, we have recently succeeded in producing magnetic nanoparticles using this technique [8, 9]. Usually, thermal annealing is required after deposition in order to enhance the alloying and to realize good crystallinity of the nanoparticles. Since the diffusion of Fe atoms into the Si substrate and a reaction between Fe and Si are necessary for the formation of iron silicides from Fe-deposited Si substrates, the heating rate during annealing is one of the important parameters controlling the morphology of iron silicide thin films. In this study we have synthesized iron silicide thin films using an electron-beam evaporation technique followed by thermal annealing with different heating rates, and characterized them by means of transmission electron microscopy (TEM).

2. Experimental procedures

Chemically etched Si(111) substrates were baked in a deposition chamber at a temperature of 823 K for 1 h to clean the surface. Then an Fe thin film with a thickness of 2 nm was deposited on the substrate in a vacuum of 10^{-6} Pa at 773 K. An amorphous Al$_2$O$_3$ film with a thickness of 3 nm was further deposited to protect the Fe thin film from oxidation. The as-deposited specimens were then annealed at 1073 K for 2 h at a vacuum of 10^{-5} Pa, using an induction heating vacuum furnace for large heating rates (~2000 K/min from room temperature

---

*Author to whom all correspondence should be addressed.

0022-2461 © *2006 Springer Science + Business Media, Inc.*
DOI: 10.1007/s10853-006-7820-0

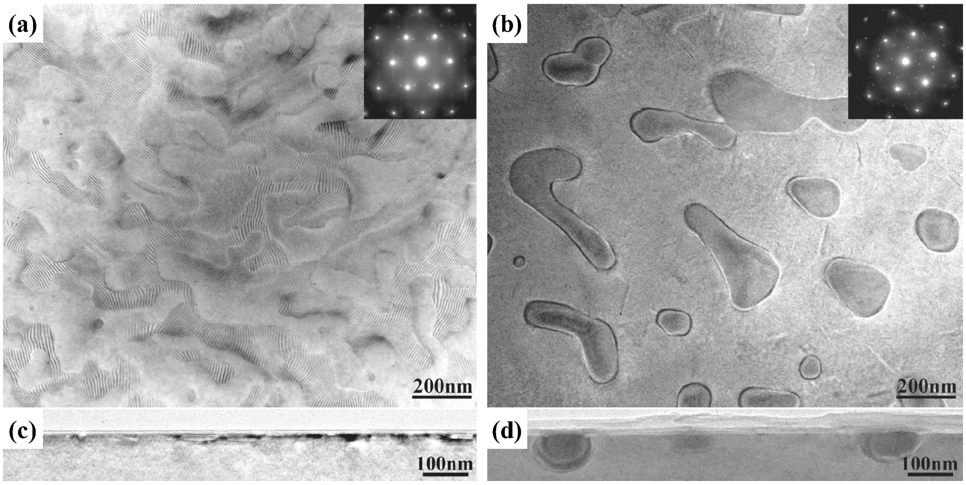

Figure 1 Bright-field TEM images of the samples annealed at 1027 K for 2 h with (a), (c) large and (b), (d) small heating rates. Selected-area electron diffraction patterns are shown in the inset. Plan-view images taken along the $[111]_{Si}$ direction reveal a quite different morphology: a discontinuous layer is formed in (a), while homogeneously dispersed nanoparticles are observed in (b). Cross-section images (c) and (d) indicate that the diffusion length of Fe atoms into a Si substrate is different between (c) and (d).

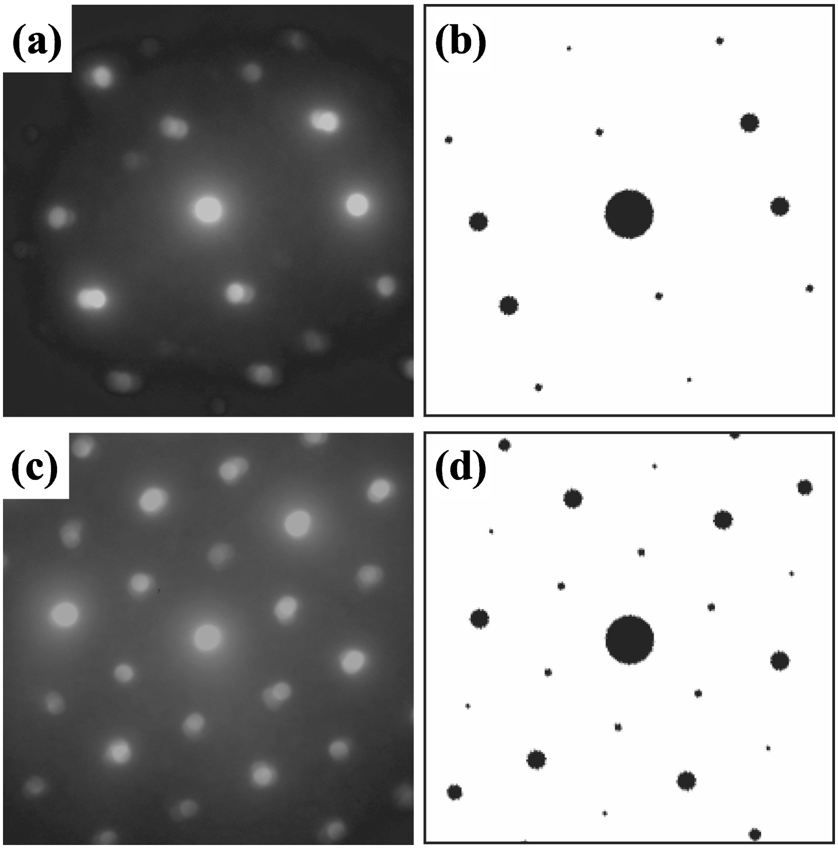

Figure 2 NBED patterns obtained from (a) cross-sectional and (b) plan-view directions of the sample annealed with rapid heating. These NBED patterns are consistent with (b) $(11\bar{3})$ and (d) $(11\bar{1})$ diffraction patterns of the ε-FeSi phase.

to 923 and ∼100 K/min from 923 to 1073 K) and using a conventional vacuum furnace for small heating rates (∼5 K/min).

The specimens obtained here were characterized using a JEOL JEM-3000F TEM with an accelerating voltage of 300 kV. Plan-view and cross-sectional TEM specimens were prepared using a combination of mechanical polishing and ion thinning with 2.5 keV Ar^+ ions. Nano-beam electron diffraction (NBED) was employed to determine the phases of the nanoparticles.

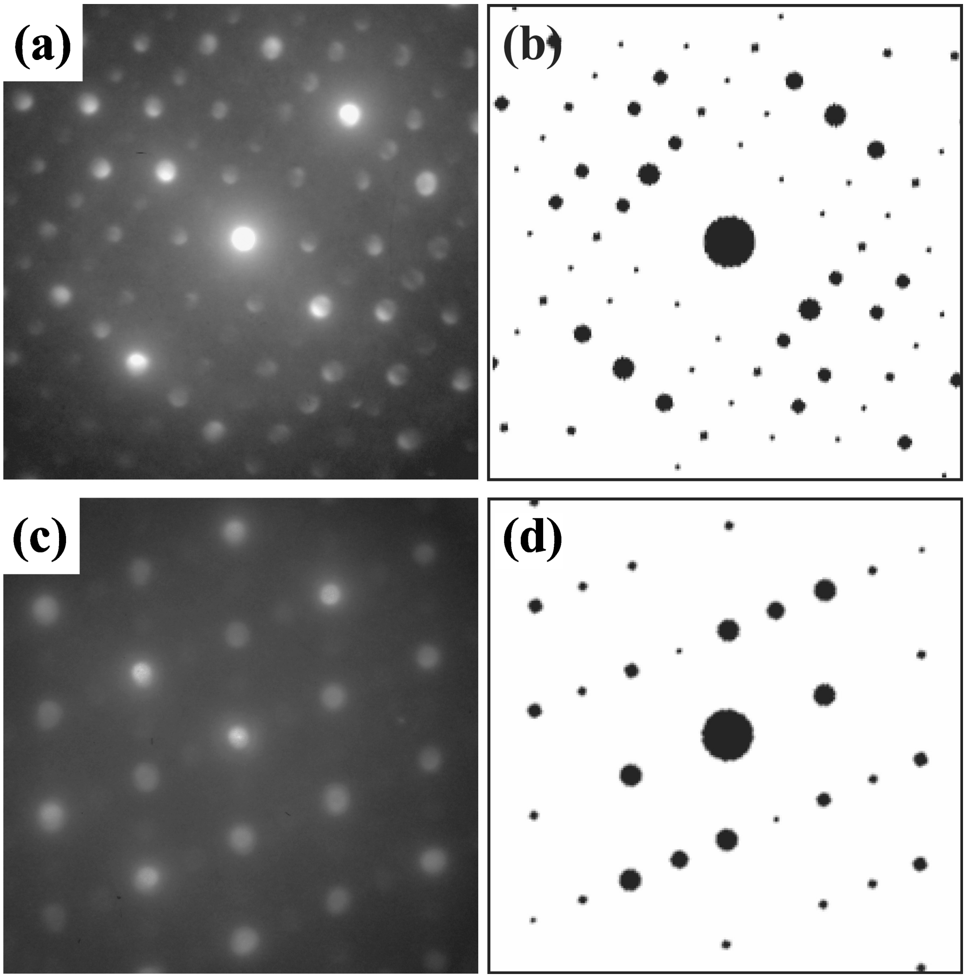

Figure 3 NBED patterns obtained from (a) cross-sectional and (b) plan-view directions of the sample annealed with slow heating. These NBED patterns are consistent with (b) ($\bar{1}10$) and (d) ($1\bar{1}1$) diffraction patterns of the β-FeSi$_2$ phase.

3. Results and discussion

Examination of the as-deposited specimen showed that Fe particles deposited on the Si(111) substrate form an iron monosilicide (ε-FeSi) film with a thickness of $\sim$3 nm (not shown). This result reveals that a substrate temperature of 773 K is still too low to form β-FeSi$_2$ nanoparticles. Fig. 1 shows (a), (b) plan-view and (c), (d) cross-sectional bright-field TEM images of specimens annealed at 1073 K for 2 h. The specimens were annealed with (a), (c) large and (b), (d) small heating rates. The cross-section images reveal the formation of small nanoparticles and plate-like compounds just beneath the surface of the Si substrate, suggesting that the deposited Fe particles diffuse significantly into the substrate. It should be noted that the thickness of the iron silicides product in Fig. 1c is smaller than that in Fig. 1d. From the plan-view images, it is apparent that the microstructures depend strongly on the heating rate. That is, a discontinuous film containing moiré fringes is observed in the specimen obtained by rapid heating, while complete separated particles with a size of $\sim$100 nm are homogeneously dispersed in the sample generated by slow heating. In addition to diffraction spots from Si with the zone axis of [111], extra spots due to iron silicides are observed in the SAED patterns (see the inset of Fig. 1a and b). These extra spots also show symmetries, suggesting that the silicides are epitaxially grown on the Si substrate.

Figs 2 and 3 show examples of NBED patterns of the specimens annealed with rapid and slow heating, respectively. These NBED patterns were taken with a probe size of $\sim$10 nm. All NBED patterns exhibit a net pattern, but their arrangements are different. To determine the crystal structure of the annealed samples, the structure factor, F_{hkl}, where hkl represents a specific Bragg reflection, was calculated for several Fe–Si compounds. Calculations of the electron diffraction patterns were based on the kinematical approximation, $F_{hkl} = \sum f_n \exp[2\pi i(hx_n + ky_n + lz_n)]$, where f_n is the atomic scattering factor for atom n at a fractional coordination (x_n, y_n, z_n). Based on these calculations, we found the NBED patterns in Fig. 2a and c are consistent with the ($11\bar{3}$) and ($11\bar{1}$) reciprocal lattice planes, respectively, of

ε-FeSi (Fig. 2b and d). On the other hand, Fig. 3a and c correspond to the patterns of β-FeSi$_2$ with the zone axes of $[\bar{1}10]$ and $[1\bar{1}1]$ (Fig. 3b and d).

We have also observed specimens annealed for 12 h and found that no differences in morphology and dominant phase comparing with 2 h-annealed samples. This suggests that heating rate rather than heating time on thermal annealing plays an important role for the phase selection during the formation of iron silicides. Two dominant processes exist in the formation of iron silicides: the diffusion of Fe atoms into the Si substrate and the reaction between Fe and Si. As described above, iron silicides in the specimen annealed with rapid heating exist in the shallower region from the substrate surface than these obtained with slow heating (see Fig. 1c and d). This suggests that in the case of the former, Fe atoms do not have enough time to diffuse into Si substrate; the Fe content is higher and the reaction between Fe and Si occurs near the substrate surface. As a result, ε-FeSi is formed. On the contrary, it is more feasible to form β-FeSi$_2$ phase because the small heating rate helps deposited Fe atoms to diffuse into the Si substrate and to interact during the increase in temperature. This means that a small heating rate is more effective to synthesize β-FeSi$_2$.

4. Conclusions

TEM investigation has been performed to clarify the effect of heating rate on the formation of iron silicides grown by an electron-beam evaporation technique. The annealed sample with a large heating rate formed a discontinuous thin film of ε-FeSi, while the sample annealed with a small heating rate showed completely separated nanoparticles with the phase of β-FeSi$_2$. The differences in the microstructures can be explained in terms of the balance between the diffusion rate of Fe atoms in Si and the reaction rate of Fe and Si. Our results suggest that the diffusion of Fe atoms into Si substrate and reaction between Fe and Si can be controlled by changing the heating rate during annealing, and we show that a slow heating rate is more effective in forming β-FeSi$_2$ nanoparticle.

References

1. M. C. BOST and J. E. MAHAN, *J. Appl. Phys.* **64** (1986) 2034.
2. N. E. CHRISTENSEN, *Phys. Rev. B* **42** (1990) 7148.
3. M. C. BOST and J. E. MAHAN, *J. Appl. Phys.* **58** (1986) 2696.
4. D. GERTHSEN, K. RADERMACHER, CH. DIEKER and S. MANTL, *ibid.* **71** (1992) 3788.
5. D. LEONG, M. HARRY, K. J. REESON and K. P. HOMEWOOD, *Nature* **387** (1997) 686.
6. S. J. CLARK, H. A. AL-ALLAK, S. BRAND and R. A. ABRAM, *Phys. Rev. B* **58** (1998) 10389.
7. D. B. MIGAS and L. MIGLIO, *ibid.* **62** (2000) 11063.
8. K. SATO, T. KAJIWARA, M. FUJIYOSHI, M. ISHIMARU, Y. HIROTSU and T. SHINOHARA, *J. Appl. Phys.* **93** (2003) 7414.
9. B. BIAN, K. SATO and Y. HIROTSU, *Appl. Phys. Lett.* **75** (1999) 3686.